Acta Biochim Biophys Sin 2011, 43: 957–969 | © The Author 2011. Published by ABBS Editorial Office in association with Oxford University Press on behalf of the Institute of Biochemistry and Cell Biology, Shanghai Institutes for Biological Sciences, Chinese Academy of Sciences. DOI: 10.1093/abbs/gmr098.

Original Article

Dihydrofolate reductase is required for the development of heart and outflow tract in zebrafish

Shuna Sun[1], Yonghao Gui[1*], Qiu Jiang[2], and Houyan Song[2]

[1]Children's Hospital, Fudan University, Shanghai 201102, China
[2]Department of Molecular Genetics, Shanghai Medical College and Key Laboratory of Molecular Medicine, Ministry of Education, Fudan University, Shanghai 200032, China
*Correspondence address. Tel/Fax: +86-21-64931990; E-mail: yhgui@shmu.edu.cn

Folic acid is very important for embryonic development and folic acid inhibition can cause congenital heart defects in vertebrates. Dihydrofolate reductase (DHFR) is a key enzyme in folate-mediated metabolism. The dysfunction of DHFR disrupts the key biological processes which folic acid participates in. *DHFR* gene is conserved during vertebrate evolution. It is important to investigate the roles of *DHFR* in cardiac developments. In this study, we showed that *DHFR* knockdown resulted in the abnormal developments of zebrafish embryos in the early stages. Obvious malformations in heart and outflow tract (OFT) were also observed in *DHFR* knockdown embryos. *DHFR* overexpression rescued the abnormal phenotypes in the *DHFR* knockdown group. *DHFR* knockdown had negative impacts on the expressions of *NKX2.5* (NK2 transcription factor-related 5), *MEF2C* (myocyte-specific enhancer factor 2C), *TBX20* (T-box 20), and *TBX1* (T-box 1) which are important transcriptional factors during cardiac development process, while *DHFR* overexpression had positive effects. *DHFR* was required for Hedgehog pathway. *DHFR* knockdown caused reduced cell proliferation and increased apoptosis, while its overexpression promoted cell proliferation and inhibited apoptosis. Taken together, our study suggested that *DHFR* plays crucial roles in the development of heart and OFT in zebrafish by regulating gene transcriptions and affecting cell proliferation and apoptosis.

Keywords dihydrofolate reductase gene; cardiac development; gene expression; Hedgehog pathway; cell proliferation; apoptosis; zebrafish

Received: May 2, 2011 Accepted: September 1, 2011

Introduction

In human, congenital cardiovascular defects occur at ~1% of the newborns, and are the commonest congenital malformations in newborns; however, the cause is not known in most cases. Recently, more and more studies, which were carried out in human and mice, have shown that folic acid plays an integral role in embryonic development and folic acid dysfunction is related to congenital heart defects [1–3]. The folate antagonists or the dysfunction of folate metabolism genes may cause heart defects, particularly ventricular septal defect and conotruncal malformations [4,5]. Risk of heart defects in infants was increased with maternal treatment using dihydrofolate reductase (DHFR) inhibitors during pregnancy [6], but this risk was reduced for women who also took folic acid supplements [7].

DHFR is a key folate metabolizing enzyme that catalyzes the reduction of folic acid into dihydrofolate. DHFR is necessary for folic acid to take part in many key biological processes. DHFR inhibition causes disruption of purine and thymidylate biosynthesis and DNA replication. In human, a 19-base pair (bp) deletion polymorphism which is a 19-bp non-coding deletion allele mapped to *DHFR* gene intron 1 is associated with increased unmetabolized folic acid in plasma and increases the risk of preterm delivery and spina bifida [8,9]. Growing awareness of the pathogenesis associated with folate deficiency contributes to the recently renewed interest in DHFR.

The zebrafish (*Danio rerio)* has emerged as a genetic and embryonical model system with several distinct advantages including external fertilization, rapid development, optical clarity of its embryos, and the ability of embryos to survive on diffused oxygen for several days without a functioning cardiovascular system. Comparison between zebrafish *DHFR* and that from other species (chicken, mice, human) (GenBank No.: zebrafish NP_571850, chicken NP_001006584, mice NP_034179, human NP_000782) indicates its conservation during evolution [**Fig. 1(A)**]. Homology is particularly high in the folate binding site and the $NADP^+$ binding site, with 70 and 88% homology with human *DHFR*, respectively [**Fig. 1(B,C)**]. The

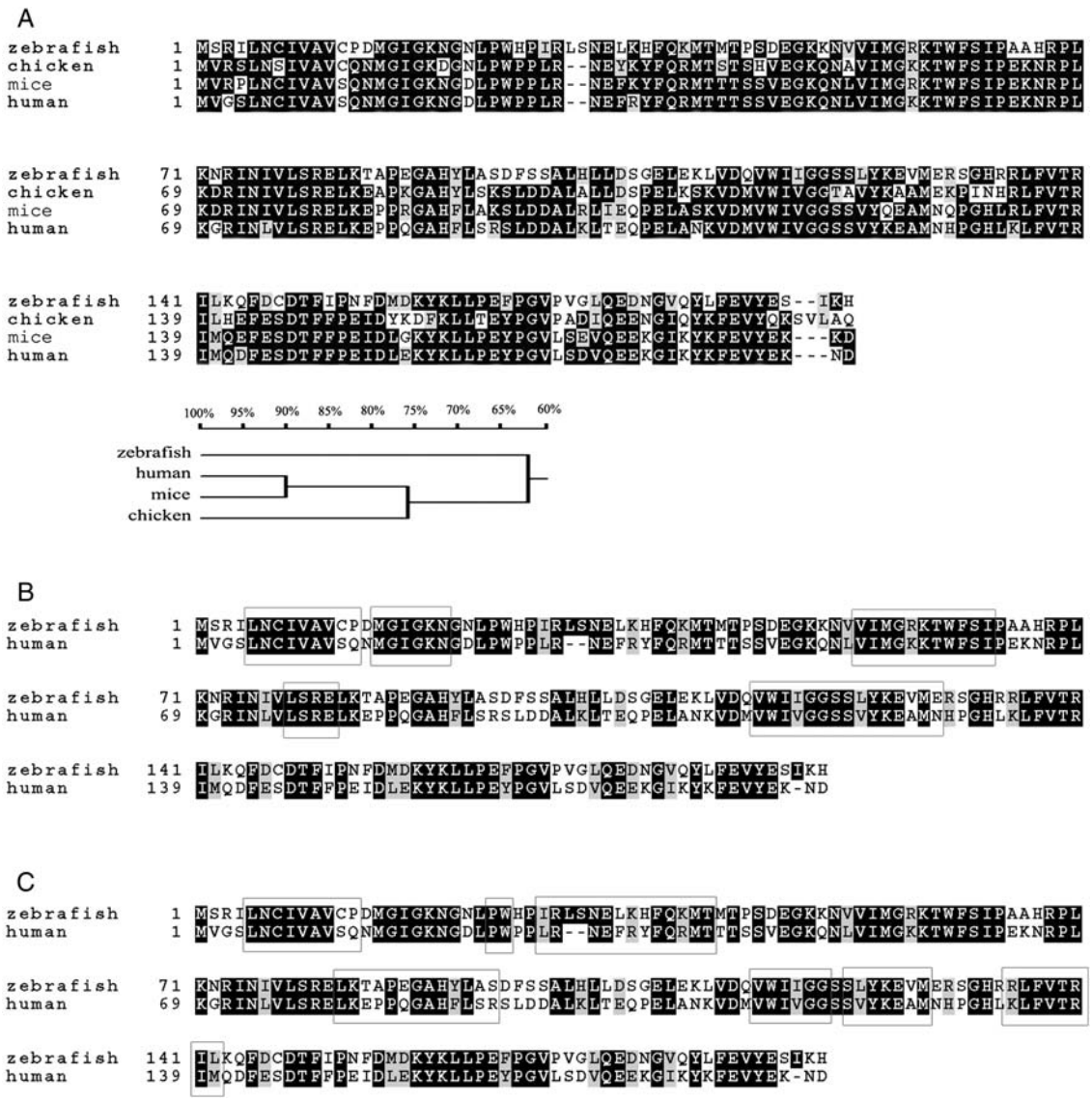

Figure 1 Comparison of DHFR amino acids in different species (A) Amino acid alignment in human, mice, chicken, and zebrafish DHFR. Note that the amino acids have high homology among different species. (B) Amino acid alignment of the $NADP^+$ binding site in humans and zebrafish. The rectangles indicate the $NADP^+$ binding site. The identity was ~88%. (C) Amino acid alignment of the folate binding site in humans and zebrafish. The rectangles indicate the folate binding site. The identity was ~70%. Gapped alignments were made by the ClustalX program.

resemblance in kinetic properties and susceptibilities to known DHFR inhibitors [e.g. methotrexate (MTX), trimethoprim] between zebrafish and human DHFRs provides the compelling evidence to support the use of zebrafish as a vertebrate model for folate-related studies. A previous investigation from our research team showed that MTX (DHFR antagonist) and *DHFR* dysfunction can affect cardiac development in zebrafish [10,11]. In MTX-treated embryos, the morphological development of ventricle and atrium was disrupted, the cardiac twist was abnormal, the heart rate and ventricular shortening fraction (VSF) were reduced, and the vascular development was disrupted. Although MTX is a well-known DHFR antagonist, whether it has other negative effects on embryonic development remains unclear. The above malformations in MTX-treated embryos may not only be caused by DHFR inhibition. Then the *DHFR* morpholino oligonucleotides (MO) microinjecting method was used to investigate the direct effects of *DHFR* dysfunction in cardiac development. *DHFR* MO can specifically and effectively knock down *DHFR* by inhibiting the translation of *DHFR*. In our previous study, the abnormal cardiac phenotypes and the reduced expression level of heart and neural crest derivatives expressed 2 gene (*HAND2)* were observed in *DHFR* MO-injected embryos [10]. But the relationship between *DHFR* and other cardiac developmental necessary factors is still not known.

Cardiac development is a tightly regulated process requiring the combinatorial interaction of multiple transcription factors and signals in a temporally and spatially

restricted fashion. The studies in flies, zebrafish, and mice have demonstrated that the transcription factors including *NKX2.5* (NK2 transcription factor-related 5), *MEF2C* (myocyte-specific enhancer factor 2C), *TBX20* (T-box 20), and *TBX1* (T-box 1) are required for appropriate heart formation, and can physically interact with many other transcriptional regulators in the cardiac developmental process [12–15]. Hedgehog signaling has an essential role in early cardiac morphogenesis, and can influence the cardiac development during later stages [16]. In this study, the effects of *DHFR* on expressions of above factors were detected.

In this work, we showed that in *DHFR* knockdown embryos, the epibolic movement was abnormal in the early stage and the cardiac and outflow tract (OFT) were dysplastic. We also revealed that *DHFR* overexpression rescued the abnormal phenotypes in the *DHFR* knockdown group. *DHFR* knockdown had negative impacts on expressions of *NKX2.5*, *MEF2C*, *TBX20*, and *TBX1*, while *DHFR* overexpression had positive effects. *DHFR* was required for the Hedgehog pathway. *DHFR* knockdown caused the reduced cell proliferation and the increased apoptosis. *DHFR* overexpression promoted the cell proliferation and inhibited the apoptosis. Together, these findings implicated that *DHFR* was a key factor in embryogenesis and cardiac development in zebrafish by regulating the transcriptions of genes and affecting cell proliferation and apoptosis.

Materials and Methods

Zebrafish strains and maintenance

Wild-type zebrafish stocks were obtained from Oregon University (Eugene, USA). The breeding facility was introduced from Aquatic Habitats Corporation (Apopka, USA). Embryos were obtained from natural spawning of wild-type adults. All fish and embryos were bred, raised, and staged in our laboratory according to previously described procedures [17]. Embryo age was defined as hours post-fertilization (h.p.f.). Embryos used for *in situ* hybridization (raised beyond 24 h.p.f.) were treated with 0.003% phenylthiourea to prevent pigmentation.

Construction of the plasmid *DHFR–GFP* and microinjections

Briefly, the *DHFR–GFP* construct was generated by fusing the fragment of *DHFR* which contains 5′ UTR (5′ non-translated region) and the start site sequence of *DHFR* (GenBank No. NM_131775) containing the coding sequence that was the target of *DHFR* MOs, in-frame into vector pEGFP-N1 (CLONTECH Laboratories, Inc., Palo Alto, USA). The construct was linearized and dissolved in Tris buffer (5 mM Tris-HCl, pH 8.0, 200 mM KCl, 0.05% phenol red) to a final concentration of 50 μg/ml. About 6 nl of sample was microinjected into the cytoplasm of the one- to two-cell-stage embryos.

DHFR–GFP and *DHFR* mRNAs syntheses and microinjections

Sense-capped *DHFR–GFP* mRNA and *DHFR* mRNA were synthesized using the mMESSAGE mMACHINE system (Ambion, Austin, USA) from the following linearized plasmids: pT7TS-*DHFR–GFP* and pT7TS-*DHFR* (zebrafish *DHFR*, digested with Bal II, transcribed with T7) [11]. RNAs were diluted to 40 μg/ml in solution A (0.1% phenol red, 0.2 M KCl), and 6 nl of *DHFR–GFP* mRNA and *DHFR* mRNA were microinjected into the cytoplasm of the one- to two-cell-stage embryos.

MO oligonucleotides microinjection

Two *DHFR* MOs (MO1 and MO2) targeting the translation initiation site and the standard control MO (Con MO) were designed (Gene Tools, Philomath, USA). MO1 targeted bases 14–38 of the zebrafish *DHFR* mRNA sequence, and MO2 targeted bases 43–67 of the zebrafish *DHFR* mRNA sequence. Sequences were as follows: MO1, 5′-ACGGTCTCGCCTTCTTCCCGCCAAG-3′; MO2, 5′-CAGTTAACAAGTCACGCTGGCTACT-3′; Con MO, 5′-CCTCTTACCTCAGTTACAATTTATA-3′. MOs were dissolved to a stock concentration of 4 mM in 30% Danieau solution, and diluted MOs were injected into the cytoplasm of the one- to two-cell-stage embryos.

Embryos were divided into five groups: Con MO-injected group (10 ng Con MO), MOI-injected group (0.75 ng MO1 + 0.75 ng MO2), MOII-injected group (1.5 ng MO1 + 1.5 ng MO2), MOIII-injected group (3 ng MO1 + 3 ng MO2), and MOIV-injected group (5 ng MO1 + 5 ng MO2).

Fluorescent immunohistochemistry

Immunohistochemistry was carried out with phospho-histone H3 antibody staining. Rabbit anti-phospho-histone H3 (Ser10) antibody (1:200; Sigma, St Louis, USA) and goat anti-rabbit IgG-TRITC antibody (1:100; Invitrogen, Carlsbad, USA) were used. All experiments were carried out according to the manufacturer's standard protocols.

Whole-mount terminal deoxynucleotide transferase-mediated dUTP nick-end labeling (TUNEL) staining

For whole-mount TUNEL staining, embryos were fixed in 4% paraformaldehyde at 4°C overnight. They were then rinsed in phosphate-buffered saline before proceeding with TUNEL staining using an *in situ* Cell Death Detection kit (Roche; Indianapolis, USA) according to the manufacturer's instructions.

Microangiography

To monitor the development of the OFT, fluorescein (2−5 nl) was microinjected into the hearts of living zebrafish embryos at 60 h.p.f. About 2−3 min later, images of the OFT were observed on a BX61 fluorescent microscope (Olympus, Tokyo, Japan) and collected with a DP70 digital camera (Olympus).

Measurement of heart rate and analyses of ventricular contractility

After being anesthetized, living embryos were transferred to a recording chamber that contained modified Tyrode's solution (136 mM NaCl, 5.4 mM KCl, 0.3 mM NaH_2PO_4, 1.8 mM $CaCl_2$, 1 mM $MgCl_2$, 10 mM HEPES, 5 mM glucose, pH 7.3) at 48 or 72 h.p.f. Heart rates were measured under a dissecting microscope. Cardiac contractions were recorded with a video camera (TK-C 1381, JVC, Yokohama, Japan) as described [11,18]. The diastolic and systolic lengths of ventricles were measured to calculate the VSF using the following formula:

$$\mathrm{VSF} = \frac{\text{ventricular length at diastole} - \text{ventricular length at systole}}{\text{ventricular length atdiastole}}$$

Whole-mount *in situ* antisense RNA hybridization and photography

Plasmids encoding zebrafish ventricular myosin heavy chain (*VMHC*) and atrial myosin heavy chain (*AMHC*) were kindly provided by Tao Zhong (Vanderbilt University, Nashville, USA). These plasmids and other plasmids (pGEM-3zf+) containing *NKX2.5*, *MEF2C*, *TBX20*, *TBX1* (GenBank Nos. *NKX2.5* NM_131421.1, *MEF2C* NM_131312, *TBX20* NM_131506.1, *TBX1* NM_183339.1), and *DHFR* were linearized by restriction enzymes before transcription with T7 or SP6 RNA polymerase (Roche). RNA probes were synthesized and labeled with DIG (digoxigenin) according to the manufacturer's protocol.

Whole-mount RNA *in situ* hybridization using DIG-labeled antisense RNA probes was carried out on groups of 20 embryos and repeated three times according to standard procedures as described [19]. Stained embryos were examined with BX61 and SZX12 microscopes (Olympus), and photographed with a DP70 digital camera (Olympus).

RNA isolation and quantitative real-time polymerase chain reaction (Q-PCR)

Zebrafish embryos were gently anesthetized with Tricaine-S. The heart (48 h.p.f.) and OFT (60 h.p.f.) were separated with a slender vitric needle and immediately put into pre-cooled Trizol reagent (Invitrogen). After gathering ~30 samples, we instantly extracted the total RNA using Trizol reagent following the manufacturer's protocol. The total RNA from the 30 embryos in 12 h.p.f. was also extracted. The RNA samples were checked to ensure that the RNA concentrations of the control and test samples were no >10% of each other. First-strand cDNA was reverse transcribed using oligo-dT primers and MMLV reverse transcriptase (Promega Technologies, Madison, USA). The cDNA was analyzed immediately or stored at −20°C until use.

Q-PCR was done using a 7300 Real-Time PCR System (Applied Biosystems, Carlsbad, USA). The sequence-specific primers were designed using Primer Express 2.0 software (Applied Biosystems) (**Table 1**). The SYBR green method was used to quantify cDNA. The relative expression levels of each gene were computed with respect to the amount of *β-actin*. The value of expression level of each gene was divided by the amount of *β-actin* in individual cDNA samples. The specificity of each reaction was controlled by melting curve analysis. Results were analyzed by 7300 Real Time PCR System software (Applied Biosystems).

Table 1 Primer sequences

Gene	Primer sequence	
NKX2.5	F: 5′-CTTCTCTCAGGCGCAGGT-3′	R: 5′-GGATGCTGGACATGCTCGACGGA-3′
MEF2C	F: 5′-AATCCGAGGACAAATATCGC-3′	R: 5′-TTAGACTGAGGGATGGCACA-3′
TBX20	F: 5′-GCGAACGCTTTCTCCATAGC-3′	R: 5′CGGACTCCTTGTCCTTGGTTT-3′
TBX1	F: 5′-GAGACTGTGATCCCGAGGAC-3′	R: 5′-TCATGATTTGTAGCGAGCCT-3′
Foxa2	F: 5′-CAAAATGGAGGGACACGA -3′	R: 5′-CTGACCGAGGTGTAACACTCA-3′
shh	F: 5′-CAACGGAAGATCTCCACACCAT-3′	R: 5′-ACCGCCGCGTATGCCAGCA-3′
Ptc1	F: 5′-TTGTGTTCGGAGCCCTGTCT-3′	R: 5′-TTGGGTTGCGGGTCGCT-3′
ehh	F: 5′-CAGCGCTGCAAGGATAAGCT-3′	R: 5′-AACTCTCTGGCCATCTCGGTGAT-3′
β-actin	F: 5′-GTCCACCTTCCAGCAGATGT-3′	R: 5′-GAGTCAATGCGCCATACAGA-3′

Statistical analysis

Data were present as the mean ± standard deviation. Comparisons between groups were analyzed by analysis of variance (ANOVA; *t*-test with Bonferroni correction). $P < 0.05$ was considered statistically significant.

Results

Efficiency and specificity of *DHFR* knockdown by microinjecting *DHFR* MOs in zebrafish

To determine the role of *DHFR* during zebrafish embryogenesis, we knocked down *DHFR* using MOs designed against the 5′ untranslated region (*DHFR* MOs) of the zebrafish *DHFR* cDNA. The successful blockages of *DHFR* translations by *DHFR* MO1 and *DHFR* MO2 separately were proved in our previous study. To confirm the efficacy of *DHFR* MO1 + *DHFR* MO2 approach, *DHFR* MOs (1.5 ng MO1 + 1.5 ng MO2) were co-injected with a *DHFR–GFP* (green fluorescence protein gene) construct. In Con MO-injected group, *GFP* expression was not observed at 13 h.p.f. [**Fig. 2(a,e)**]. There was no detectable *GFP* knockdown when *DHFR–GFP* construct was co-injected with a random Con MO [**Fig. 2(b,f)**]. As shown in **Fig. 2**, *DHFR* MOs specifically knocked down the expression of *GFP* from the RNA transcript of the *DHFR–GFP* construct (93 ± 2.64%, $n = 100$) [**Fig. 2(c,g)**]. This result revealed the ability of the *DHFR* MOs to inhibit protein production from its target sequence.

Microinjecting *DHFR* mRNA induced *DHFR* overexpression

Green fluorescence was not observed in controls, whereas green fluorescence was detected in *DHFR–GFP* mRNA-injected groups (89 ± 3.06%, $n = 100$) [**Fig. 2(d,h)**]. This result indicated the success of *DHFR–GFP* mRNA transcription. *DHFR* mRNA was transcribed by the same technology. *DHFR* expression was detected by *in situ* antisense RNA hybridization. In controls, *DHFR* was expressed in the eyes, central nervous system, and intermediate cell mass at 19 h.p.f. [**Fig. 2(i)**]. The expression of *DHFR* in the *DHFR* mRNA-injected group was increased, indicating that microinjecting *DHFR* mRNA induced its overexpression in the transcriptional level [**Fig. 2(j)**].

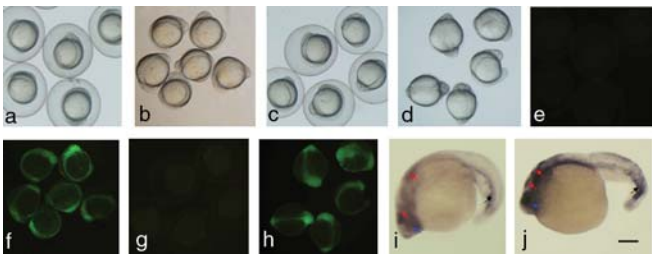

Figure 2 The effectiveness of *DHFR* knockdown and overexpression (a,e,i) Con MO-injected group. (b,f) *DHFR–GFP* construct + Con MO-injected group. (c,g) *DHFR–GFP* construct + *DHFR* MOs (MO1 1.5 ng + MO2 1.5 ng)-injected group. (d,h,j) *DHFR–GFP* mRNA-injected group. (a–d) Observed under optical microscope. (e–h) Observed under a fluorescent microscope. (i,j) The eyes (blue arrow), central nervous system (red arrows), and intermediate cell mass (black arrows). Bar: 250 μm (a–h) and 125 μm (i,j).

Classification of *DHFR* knockdown embryos

In any group, no embryo died before 22 h.p.f. All the Con MO-injected embryos developed normally. At 10 h.p.f., in normal developmental embryos, the epiboly closed as the blastoderm completely covered the yolk plug. The anterior end of the embryonic axis was thickened, which was where the head would form. The anterior–posterior (AP) angle was 180° [**Fig. 3A(a)**]. At 16 h.p.f., the yolk cell began to look like a kidney bean, heralding formation of the yolk extension. Somites began to show a chevron shape. The extending axis curled around the yolk. The entire embryo was transparent. The angle between the head and tail was ~310° [**Fig. 3A(f)**]. At 22 h.p.f., straightening of the posterior trunk was nearly complete, but the elongating tail still curved ventrally. The eyes, the otic vesicle, the brain with ventricles present along its length, and the somite with a 'V' shape were clearly observed [**Fig. 3A(k)**].

In the *DHFR* MOs-injected group, the obviously abnormal embryonic developments were observed. At 10 h.p.f., epibolic movements were abnormal. The AP angles were reduced and the posterior end of the epiboly was directed outward. The anterior end of the embryonic axis (the prospective head region) was not thickening. At 16 h.p.f., the yolk still looked like a ball without extension. The tail departed from the yolk. The somites were short and had lost the chevron shape. The body was hypogenesis and not transparent. The AP angle was reduced continuously. At 22 h.p.f., the yolk extension was half the length of the yolk ball. The trunk was short and the tail twisted and smaller. Boundaries of the somites were not distinct.

Based on the severity, the abnormal phenotypes in *DHFR* MOs-injected group were categorized into three major classes [**Fig. 3A(b,g,l;c,h,m;d,i,n)**]. Phenotypes were scored and disrupted epibolic movements, abnormal anteroposterior development, and overall hypogenesis were showed. With the microinjecting dose of MOs increasing, the malformations of embryos become more and more severe. The percentages of each class under different doses of MOs were shown in **Fig. 3(A)**. Experiments were repeated three times, numbers in pie charts were averages ($n = 100$).

Effects of *DHFR* knockdown and overexpression on cell proliferation and apoptosis

The mitotic cells were marked by phosphohistone H3 (PH3) antibody staining (red fluorescence) to test the cell

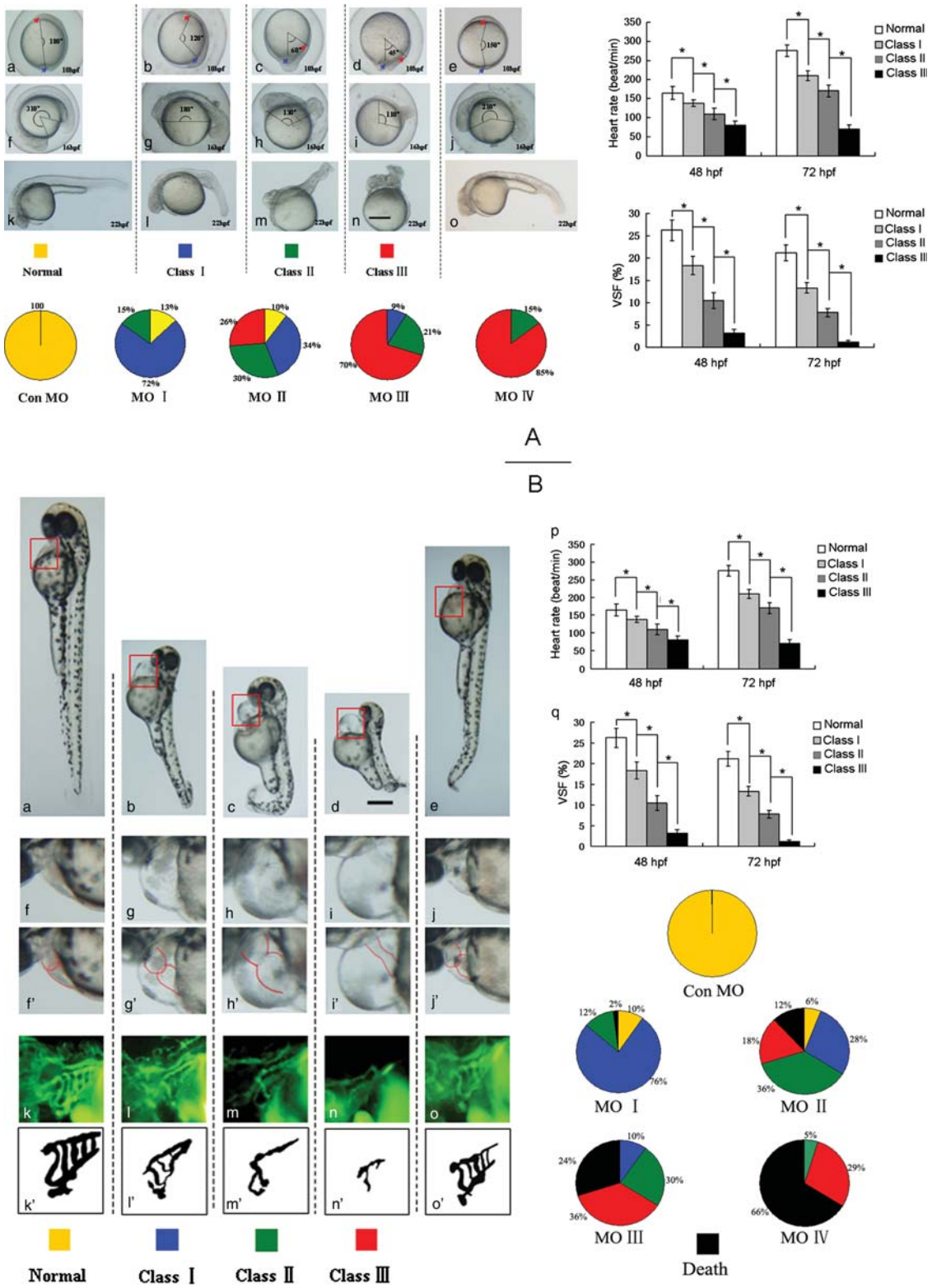

Figure 3 Development of zebrafish heart and OFT in early stages (A) The development of zebrafish in early stages. Con MO-injected embryos had normal development (a,f,k). Injection of *DHFR* MOs resulted in three classes of phenotypes. Co-injection with *DHFR* mRNA rescued the abnormal phenotypes in the *DHFR* MOII-injected group (e,j,o). (a–e) Left-lateral views, head at the top. (f–o) Left-lateral views, head to the left. Bar: 250 μm. (B) Development of the heart and OFT. (f to j′) Heart morphology. (f′–j′) Cardiac conceptual diagrams. Con MO-injected embryos had no malformations (a,f,f′,k,k′). Injection of *DHFR*-MOs induced three classes of phenotypes in live embryos. Co-injection with *DHFR* mRNA improved the developments of heart and OFT in *DHFR* MOII-injected group (e,j,j′,o,o′). (k–o) Images of OFTs detected by fluorescent microangiography at 60 h.p.f. (k′–o′) Conceptual diagrams of OFTs. (a–e) Left-lateral views of 48 h.p.f. live embryos, heads at the top. (f–j) Left-lateral views of live embryos at 48 h.p.f., heads to the left. (p, q) Analysis of heart rate and VSF. Values are mean ± standard deviation. ($n = 50$) Comparisons between groups were made with ANOVA (*t*-test with Bonferroni correction). *$P < 0.05$, compared with embryos with normal development, heart rate, and VSF gradually decreased from class I to class III. Bar: 250 μm (a–e) and 70 μm (f–j, k–o).

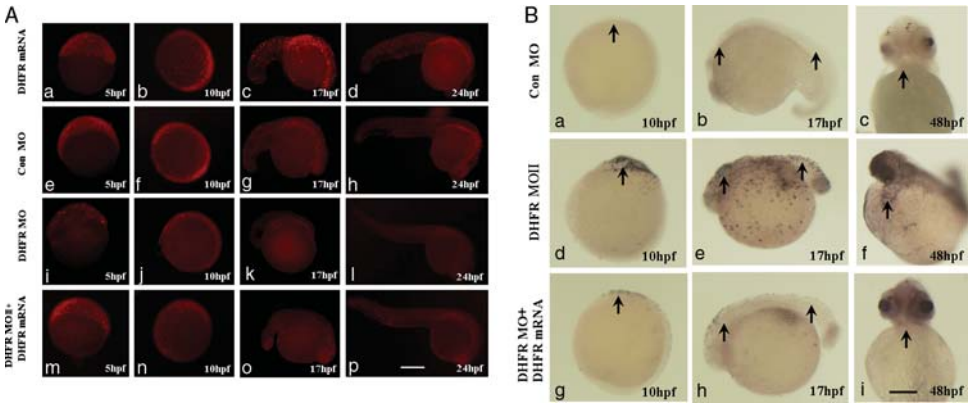

Figure 4 Cell proliferation and apoptosis (A) *DHFR* inhibition results in inhibition of cell proliferation (immunohistochemistry with phospho-histone H3 antibody staining). (a–d) *DHFR* mRNA-injected group, (e–h) Con MO-injected group, (i–l) *DHFR* MOII-injected group. (m–p) *DHFR* MOII + *DHFR* mRNA-injected group. (a,b,e,f,i,j,m,n) Heads at the top, (c,d,g,h,k,l,o,p) right-lateral views with heads to the right. Bar: 250 μm. (B) *DHFR* inhibition results in induction of apoptosis (TUNEL staining). (a–c) Con MO-injected group, (d–f) *DHFR* MOII-injected group. (g–i) *DHFR* MOII + *DHFR* mRNA-injected group. (a,d,g) Lateral views, heads at the top. (b,e,h) Left-lateral views with heads to the left. (c,f,i) Dorsal views, heads at the top. Bar: 125 μm.

proliferation in embryos. In the early stages, embryos with the decreased cell proliferation in *DHFR* MOII-injected embryos were detected (5 h.p.f., 10.0 ± 1.0; 10 h.p.f., 11.3 ± 2.1; 16 h.p.f., 11.0 ± 2.0; 24 h.p.f., 10.3 ± 1.5, $n = 20$) [**Fig. 4A(i–l)**] compared with Con MO-injected embryos [**Fig. 4A(e–h)**]. To confirm that defective cell proliferation in *DHFR* MOII-injected embryos was caused by *DHFR* loss, mRNA encoding full-length *DHFR* was co-injected with *DHFR* MOII. As shown in **Fig. 4A(m–p)**, co-injection of *DHFR* MOII along with *DHFR* mRNA resulted in significant recovery of cell proliferation (5 h.p.f., 9.7 ± 1.2; 10 h.p.f., 10.7 ± 0.6; 16 h.p.f., 9.3 ± 0.6; 24 h.p.f., 10.3 ± 1.2, $n = 20$). Comparing with Con MO-injected group, embryos with the increased cell proliferation in only *DHFR* mRNA-injected group were also detected (5 h.p.f., 11.7 ± 1.5; 10 h.p.f., 11.3 ± 0.6; 16 h.p.f., 13.0 ± 1.7; 24 h.p.f., 12.3 ± 2.5, $n = 20$) [**Fig. 4A(a–d)**].

The TUNEL assay was carried out to test the apoptosis. Compared with control embryos [**Fig. 4B(a–c)**], *DHFR* MOII-injected embryos exhibited increased apoptosis in the head at 10 h.p.f. (14.0 ± 3.0, $n = 20$) [**Fig. 4B(d)**] and in the entire body at 17 h.p.f. (12.3 ± 2.5, $n = 20$) [**Fig. 4B(e)**]. At 48 h.p.f., there was a clear increase in cell death in the heart region (14.0 ± 2.7, $n = 20$) [**Fig. 4B(f)**]. Co-injection of *DHFR* MOII along with *DHFR* mRNA partially reduced cell death in *DHFR* MOII-injected embryos (10 h.p.f., 10.0 ± 1.0; 17 h.p.f., 9.3 ± 2.3; 48 h.p.f., 9.7 ± 3.1, $n = 20$) [**Fig. 4B(g–i)**].

Effects of *DHFR* knockdown on development of the heart and the OFT

In normal embryos at 48 h.p.f., the heart tube was bending to bring the atrium into a position dorsal and left to the ventricle. The heart was beating vigorously, the heart rate was ~165 beats/min (b.p.m.) and the VSF was ~26.2%. We detected OFT development using fluorescent microangiography. In controls, the ventral aorta and AA1–AA4 (where AA1 is the mandibular arch, AA2 is the hyoid arch, AA3 is the first branchial arch, and AA4 denotes the second branchial arch) could be clearly observed. At 72 h.p.f., the heart rate increased to ~275 b.p.m. whereas the VSF was slightly reduced to ~21.2% [**Fig. 3B(a,f,f′,k,k′,p,q)**].

At 48 h.p.f., some *DHFR* MOs-injected embryos were dead due to severe malformations. Abnormal phenotypes of the heart and OFT in living embryos were divided into three classes according to severity.

For class I, compared with controls, embryos showed an expanded heart, mild pericardial edema, slow heartbeat (138 b.p.m. at 48 h.p.f. and 210 b.p.m. at 72 h.p.f.), reduced VSF (18.3% at 48 h.p.f. and 13.3% at 72 h.p.f.) and a narrow OFT [**Fig. 3B(b,g,g′,l,l′,p,q)**].

For class II, the heart was more dilated, and the pericardial sac of the embryo was continuously expanding. The heart rate (110 b.p.m. at 48 h.p.f. and 170 b.p.m. at 72 h.p.f.) and VSF (10.5% at 48 h.p.f. and 7.8% at 72 h.p.f.) were further reduced than those of class I. OFT development was obviously abnormal [**Fig. 3B(c,h,h′,m,m′, p,q)**].

For class III, the heart was a straight tube, the ventricle and atrium could not be clearly distinguished from each other. Pericardial edema was more severe. Heartbeats were very slow and weak. Heart rate was only 80 b.p.m. at 48 h.p.f., and 70 b.p.m. at 72 h.p.f. The VSF was only 3.2% at 48 h.p.f. and nearly zero at 72 h.p.f. OFT development displayed considerable hypogenesis, only few parts of the OFT were observed [**Fig. 3B(d,i,i′,n,n′,p,q)**].

In *DHFR* MOs-injected groups, the prevalence and severity of abnormalities of the heart and OFT directly correlated with MO dose as shown in **Fig. 3(B)**. *DHFR*

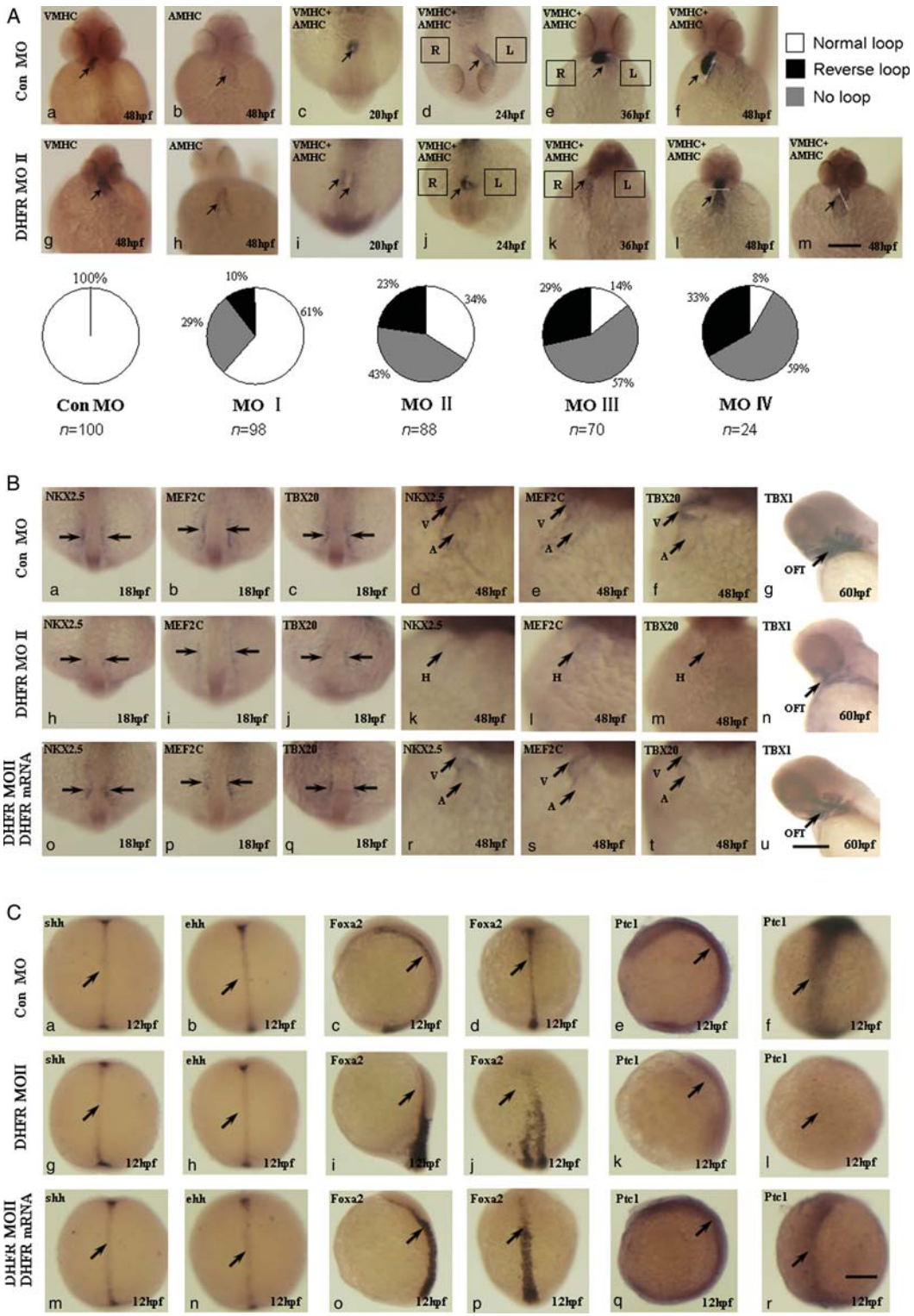

Figure 5 Expression of genes detected by *in situ* hybridization (A) The expression pattern of *VMHC* and *AMHC* detected by *in situ* hybridization. (a–f) Con MO-injected group. (g–m) *DHFR* MOII-injected group. In *DHFR* MOII-injected embryos, the heart tubes were abnormally looped at 48 h.p.f. (l and m) including no loop and adverse loop. The proportion of abnormal loops in groups with different microinjection doses of *DHFR* MOs were shown in pie charts. (c,d,i, j) Dorsal views, tails to the top. The other images were ventral views with heads to the top. R, right side; L, left side. Bar: 125 μm. (B) The expressions of *NKX2.5*, *MEF2C*, *TBX20*, and *TBX1* detected by *in situ* hybridization. (a–g) Con MO-injected group, (h–n) *DHFR* MOII-injected group. (o–u) *DHFR* MOII + *DHFR* mRNA-injected group. (a–c, h–j, o–q) Dorsal views, tails to top. (d–f, k–m, r–t) Ventral views, heads to top. (g,n,u) Left-lateral views, heads to the left. V, ventricle; A, atrium; H, heart; OFT, outflow tract. Bar: 125 μm (a–c, h–j, o–q), 70 μm (d–f, k–m, r–t), 250 μm (g, n, u). (C) The expressions of *shh*, *ehh*, *Foxa2*, and *Ptc1* (*in situ* hybridization). (a–f) Con MO-injected group. (g–l) *DHFR* MOII-injected group. (m–r) *DHFR* MOII + *DHFR* mRNA-injected group. (c,i,o,e,k,q) Left-lateral views, head to the top. The other images were dorsal views with heads to the top. Bar: 125 μm.

MOs-injected embryos all died 5 days after fertilization. Due to the relative majority of abnormal phenotypes and the relative minority of deaths, embryos microinjected with *DHFR* MOII were used to do the following experiment.

DHFR overexpression rescued the abnormal phenotypes in the *DHFR* knockdown group

Comparing with *DHFR* MOII-injected group, the development of embryos in early stages and the developments of heart and OFT at 48 h.p.f. in *DHFR* mRNA + *DHFR* MOII-injected group obviously improved [**Fig. 3A(e,j,o), B(e,j,j′,o,o′)**].

Effects of *DHFR* knockdown on the expression of *VMHC* and *AMHC*

In zebrafish, the ventricle and atrium can be clearly visualized by the ventricular marker VMHC or the atrial marker AMHC. The results from *in situ* hybridization with *VMHC* or *AMHC* at 48 h.p.f. showed that in *DHFR* MOII-injected group [**Fig. 5A(g,h)**], the expression of *VMHC* and *AMHC* had no obvious differences compared with those in controls [**Fig. 5A(a,b)**].

Results from the *in situ* hybridization with *VMHC* + *AMHC* showed that in the Con MO-injected group, the primitive heart tubes on each side of the midline fused to form the circular heart tube at 20 h.p.f. [**Fig. 5A(c)**]. Formed a linear shape and moved to the left at 24 h.p.f. [**Fig. 5A(d)**].The bend of the heart was prominent and the division between the atrium and ventricle was marked at 36 h.p.f. [**Fig. 5A(e)**]. Cardiac looping was complete and the atrium was dorsal and left to the ventricle at 48 h.p.f. [**Fig. 5A(f)**].

In some *DHFR* MOII-injected embryos, the primitive heart tubes were not fusing at 20 h.p.f. (17 ± 1, $n = 20$) [**Fig. 5A(i)**], formed irregular circular heart tubes at 24 h.p.f. (16 ± 3, $n = 20$) [**Fig. 5A(j)**], developed to the right side at 36 h.p.f. (13 ± 2, $n = 20$) [**Fig. 5A(k)**], and were abnormally looped at 48 h.p.f. The abnormal loop included no loop (8.6 ± 1.5, $n = 20$) [**Fig. 5A(l)**] and an adverse loop (4.6 ± 0.6, $n = 20$) [**Fig. 5A(m)**]. With increasing doses of MOs, the percentage of live embryos with abnormal loops was enhanced and the proportion of adverse loops increased. The absence of cardiac fusion at 20 h.p.f. was due to the developmental delay as no cardia bifida phenotype was observed at later stages.

Effects of *DHFR* knockdown and overexpression on the expressions of *NKX2.5*, *MEF2C*, *TBX20*, and *TBX1*

The results of *in situ* hybridization showed that in controls, *NKX2.5*, *MEF2C*, and *TBX20* were expressed in heart primordia at 18 h.p.f. [**Fig. 5B(a−c)**], and strong expressions of these genes were observed in the entire heart at 48 h.p.f. [**Fig. 5B(d−f)**]. Compared with controls, the expression of *NKX2.5*, *MEF2C*, and *TBX20* in *DHFR* MOII-injected embryos decreased in heart primordia at 18 h.p.f. (*NKX2.5* 13.3 ± 1.5, *MEF2C* 16.7 ± 2.1, *TBX20* 15.3 ± 2.5, $n = 20$) [**Fig. 5B(h−j)**] and decreased in the atrium and ventricle at 48 h.p.f. (*NKX2.5* 14.7 ± 1.5, *MEF2C* 15.7 ± 0.6, *TBX20* 16.3 ± 2.1, $n = 20$) [**Fig. 5B(k−m)**]. In controls at 60 h.p.f., the expression of *TBX1* was clearly visible in the OFT [**Fig. 5B(g)**]. Compared with controls, the expression of *TBX1* in *DHFR* MOII-injected embryos was reduced (12.7 ± 1.2, $n = 20$) [**Fig. 5B(n)**]. The results of real-time PCR also demonstrated that in the *DHFR* MOII-injected group, the expression of *NKX2.5*, *MEF2C*, and *TBX20* decreased at 48 h.p.f. in the heart. The expression of *TBX1* detected by real-time PCR at 60 h.p.f. in the OFT was also lower than those in the controls (**Table 2**).

Embryos microinjected with *DHFR* mRNA plus *DHFR* MOII showed increased expressions of *NKX2.5*, *MEF2C*, and *TBX20* in heart primordia (*NKX2.5* 11.3 ± 3.2, *MEF2C* 11.7 ± 2.1, *TBX20* 13.0 ± 3.0, $n = 20$) [**Fig. 5B(o−q)**] and in the heart (*NKX2.5* 12.3 ± 0.1, *MEF2C* 13.3 ± 1.2, *TBX20* 11.3 ± 1.2, $n = 20$) [**Fig. 5B(r−t)**] than embryos microinjected with *DHFR*

Table 2 Relative expression levels of genes detected by real-time PCR

Group	Gene							
	NKX2.5	*MEF2C*	*TBX20*	*TBX1*	*shh*	*ehh*	*Foxa2*	*Ptc1*
Con MO	1.00 ± 0.10	1.23 ± 1.15	0.73 ± 0.15	0.55 ± 0.10	1.03 ± 0.25	1.20 ± 0.10	1.25 ± 0.13	1.47 ± 0.15
DHFR MOII	0.42 ± 0.06^{a}	0.61 ± 0.08^{a}	0.41 ± 0.10^{a}	0.21 ± 0.04^{a}	0.90 ± 0.1^{b}	1.13 ± 0.13^{b}	1.27 ± 0.25^{b}	0.68 ± 0.10^{a}
DHFR MOII + *DHFR* mRNA	0.63 ± 0.08^{c}	0.83 ± 0.03^{c}	0.67 ± 0.12^{c}	0.42 ± 0.08^{c}	1.01 ± 0.1^{d}	1.08 ± 0.23^{d}	1.15 ± 0.05^{d}	1.10 ± 0.10^{c}

[a] $P < 0.05$, compared between Con MO-injected group and *DHFR* MOII-injected group.
[b] $P > 0.05$, compared between Con MO-injected group and *DHFR* MOII-injected group.
[c] $P < 0.05$, compared between *DHFR* MOII-injected group and *DHFR* MOII + *DHFR* mRNA-injected group.
[d] $P > 0.05$, compared between *DHFR* MOII-injected group and *DHFR* MOII + *DHFR* mRNA-injected group.

MOII. Increased expression of *TBX1* in the OFT was also observed (11.0 ± 2.0, $n = 20$) [**Fig. 5B(u)**]. The results of real-time PCR confirmed that after being microinjected with both *DHFR* mRNA and *DHFR* MOII, embryos had increasing expressions of *NKX2.5*, *MEF2C*, *TBX20*, and *TBX1* than those microinjected with *DHFR* MOII alone (**Table 2**).

Effects of *DHFR* knockdown and overexpression on the Hedgehog pathway

Shh (sonic hedgehog a) and *ehh* (indian hedgehog homolog b) are two Hedgehog genes. *Foxa2* (forkhead box A2) and *Ptc1* (patched 1) are members of the Hedgehog pathway, and are sensitive targets of Hedgehog signaling. Whole-mount *in situ* hybridization analysis showed that *shh* and *ehh* were expressed at the midline in the early embryonic stages [**Fig. 5C(a,b)**]. Expressions of these two Hedgehog genes appeared to be normal in *DHFR* MOII-injected embryos at 10 h.p.f. [**Fig. 5C(g,h)**]. In controls at 10 h.p.f., *Foxa2* and *Ptc1* expressed in axes [**Fig. 5C(c–f)**]. In *DHFR* MOII-injected embryos, the expression intensity of *Foxa2* was not affected. But the *Foxa2* expression in the anterior axis of *DHFR* MOII-injected embryos was totally absent, and *Foxa2* expression in the posterior axis expanded to both sides (13.3 ± 1.5, $n = 20$) [**Fig. 5C(i,j)**]. The expression of *Ptc1* (a sensitive target of Hedgehog signaling) was decreased in *DHFR* MOII-injected embryos (14.7 ± 2.5, $n = 20$) [**Fig. 5C(k,l)**]. Compared with the group microinjected with *DHFR* MOII alone, in the group microinjected with *DHFR* mRNA plus *DHFR* MOII, the expressions of *shh*, *ehh*, and *Foxa2* showed no differences [**Fig. 5C(m–p)**], whereas the expression of *Ptc1* was clearly increased (16.3 ± 2.1, $n = 20$) [**Fig. 5C(q,r)**]. *Foxa2* was expressed in the anterior and posterior axis in embryos microinjected with *DHFR* mRNA plus *DHFR* MOII (12.0 ± 1.7, $n = 20$) [**Fig. 5C(o,p)**].

The results of real-time PCR also demonstrated that the expression of *Ptc1* decreased and the expressions of *shh*, *ehh*, and *Foxa2* were not significantly different at 12 h.p.f. in the *DHFR* MOII-injected group compared with those in the controls. In the *DHFR* MOII + *DHFR* mRNA-injected group, the expression of *Ptc-1* was increased compared with that in the *DHFR* MOII-injected group (**Table 2**).

Discussion

Fish has a two-chambered heart in which a single-loop circulatory pattern takes blood from the heart to the gills and then to the body. Mammals have a four-chambered heart, with complete separation of both systemic and pulmonary circuits. Although the anatomy of hearts in fish and mammals is different, the comparison between zebrafish *DHFR* and that from other species (chicken, mice, human) indicates conservation during evolution and the homology of functional domains of *DHFR* are particularly high. In addition, zebrafish offers several distinct advantages as an embryological and genetic model system. Zebrafish embryos are not completely dependent on a functional cardiovascular system. Even in the total absence of blood circulation, they receive enough oxygen by passive diffusion to survive, thereby allowing a detailed analysis of animals with severe cardiovascular defects. Therefore, zebrafish was used in this study to investigate the roles of *DHFR* in embryonic and cardiac developments.

DHFR is abundant in zebrafish embryos in the early stages and decreases abruptly 3 days after fertilization. In zebrafish, from 1 to 4 somites (10.33 h.p.f.) to long-pec stage (48 h.p.f.), *DHFR* is expressed in the entire organism (in the neural plate, tail bud, central nervous system, intermediate cell mass of mesoderm, optic tectum, retina, pectoral fin musculature, heart, muscle, liver, spleen, spinal cord, and pharyngeal arch, see http://zfin.org, ZFIN ID: ZDB-FIG-050630–6067, 128, 6110, 2433, 7081). In this study, the blocked expression approach coupled with overexpression experiments was used to investigate the function of *DHFR*. The MOs was used to block the translation of *DHFR* mRNA followed by knockdown of *DHFR*. MOs have been investigated in many studies as an effective means to inhibit gene function in embryos. The evidence suggests that MOs provide a relatively simple, promising approach and rapid method to study gene function *in vivo*. The MOs used to knock down *DHFR* in this study were designed and synthesized by Gene Tools. They can effectively stop *DHFR* translation. The co-injection of MOs with *DHFR–GFP* construct demonstrated that *DHFR* MOs inhibited the production of the DHFR–GFP fusion protein, indicating that *DHFR* MOs could efficiently knock down the *DHFR*.

The *DHFR* knockdown embryos showed disrupted epibolic movements and abnormal AP development at 10 h.p.f., and the overall malformations appeared with embryonic maturity. *DHFR* overexpression could rescue these malformations. These results indicated that *DHFR* had an important role in embryonic development in the very early stages. The phenotypes of *DHFR* knockdown embryos in early stages were described in detail and were expected to provide important clues to further investigations about how *DHFR* takes part in the early embryonic development.

DHFR is essential for the metabolism and growth of cells. *DHFR* inhibition may result in DNA instability and the reduced cell proliferation. We detected apoptosis and cell proliferation using TUNEL assay, which is a method

for detecting DNA breakage by labeling the terminal end of nucleic acids, and immunohistochemistry with the PH3 antibody staining protocol. Histone H3 (mitosis marker) is specific for phosphorylated histone H3 (17 kDa) and has been reported to detect mitotic cells in *Caenorhabditis elegans* and *Drosophila* embryos by immunohistochemistry. In this study, reduced cell proliferation and excessive apoptosis were detected in *DHFR* knockdown embryos at the early stages of development. Overexpressing *DHFR* mRNA alone was performed and the increased proliferation was detected, which support the conclusion that *DHFR* can promote proliferation.

Multiple malformations of the heart and OFT were generated in *DHFR* knockdown embryos. The ventricle and atrium had abnormal morphogenesis and an abnormal position, the abnormal heart had weak systole, and heart rate and VSF were clearly reduced. The abnormal OFT was also detected by using fluorescent microangiography. Zebrafish *VMHC* stands for the ventricular myosin heavy chain gene, and *AMHC* stands for the atrium myosin heavy chain gene; both genes have important roles in the differentiation and function of ventricular and auricular myocardiocytes [19]. *VMHC* and *AMHC* were used as the specific markers to label the ventricle and atrium. In *DHFR* knockdown embryos, although the expressions of *VMHC* and *AMHC* appeared normal, the results of *VMHC* + *AMHC in situ* hybridization showed delayed development of the heart, cardiac dystopia to the right side, and abnormal cardiac looping. These abnormal developments became progressively more severe with increasing doses of *DHFR* MOs. *DHFR* overexpression rescued the abnormal cardiac phenotypes of *DHFR* knockdown embryos. These results demonstrated that *DHFR* had important roles in the heart and OFT developments. To further investigate *DHFR* functions during the developmental process of the heart and OFT, the expression of genes which are important for cardiac development or participate in the Hedgehog pathway were detected by *in situ* hybridization and real-time PCR.

NKX2.5 is the conserved transcription factor and a central component of the transcription factor network that guides cardiac development [12,20] and is essential for normal heart morphogenesis, myogenesis, and function [21]. Mutations of *NKX2.5* are associated with congenital heart diseases in humans [22]. *MEF2C* belongs to the MEF2 family, which is the muscle-enriched transcription factor that bounds to an A/T-rich DNA sequence in the control regions of numerous muscle-specific genes and is essential for differentiation of cardiac muscle [13,23]. MEF2 dysfunction causes dilated cardiomyopathy, lengthening of myocytes, and disrupted regulation of cardiac energy metabolism during cardiac development. *TBX1* and *TBX20* are members of the T-box family of transcriptional regulators, and have been implicated in the regulation of heart development in several vertebrate species. *TBX1* is the major gene underlying del22q11.2 or the DiGeorge syndrome in humans. It is required for the formation of OFT and is also necessary for asymmetric cardiac morphogenesis [14,24–26]. Loss of *TBX20* results in defects in heart formation, including OFT hypoplasia and decreased expression of *NKX2.5* and *MEF2C* [15,27,28]. In zebrafish, the earliest expression of *NKX2.5* in heart primordia was detected at one to four somites (10.33 h.p.f.) (http://zfin.org, ZFIN ID: ZDB-FIG-090218-993). *MEF2C* and *TBX20* were first expressed in the heart primordial at 14–19 somites (16 h.p.f.) (http://zfin.org, ZFIN ID: ZDB-FIG-060710–739, ZDB-FIG-050630–7479) which was later than *NKX2.5*. By 51 h.p.f., *TBX1* expression could be seen in cardiac OFT. *NKX2.5* therefore participates in the early stage, *MEF2C* and *TBX20* are involved in the middle stage, and *TBX1* take part in the later period of cardiac development.

The Hedgehog pathway is crucial for normal OFT development [16,29]. In the absence of *Shh*, the cardiac phenotype results from arch artery and OFT patterning defects [30]. Hedgehog signaling is also required for the induction of left-side determinants. Left–right asymmetry of the heart and visceral organs in vertebrates is regulated by the Hedgehog pathway. In the mouse embryo, the Hedgehog pathway is required to prevent left determinants from being expressed on the right. In zebrafish, Hedgehog signals influence the development of multiple organ asymmetries [31].

Due to the central roles of *NKX2.5*, *MEF2C*, *TBX1*, *TBX20*, and the Hedgehog pathway in heart formation, OFT development and left–right asymmetry of heart, the expressional levels of these genes were detected in *DHFR* knockdown embryos. We found that in *DHFR* knockdown embryos, decreased expression of *NKX2.5*, *MEF2C*, *TBX1*, *TBX20*, and *Ptc-1* was detected.

To prove that *DHFR* has positive effects on the expression of *NKX2.5*, *MEF2C*, *TBX1*, *TBX20*, and *Ptc-1*, and to confirm that *DHFR* can promote cell proliferation and inhibit apoptosis, the *DHFR* overexpression experiment was designed. *DHFR–GFP* mRNA was synthesized *in vitro*. The strong green fluorescence, observed in the *DHFR–GFP* mRNA-injected group, indicated that the expressions of DHFR and GFP *in vivo*. *DHFR* mRNA was synthesized and microinjected with the same technologies. In the *DHFR* mRNA-injected group, the expression of *DHFR* which was detected by *in situ* hybridization was increased. The above results confirmed the success of *DHFR* overexpression. Our results revealed that in *DHFR* knockdown embryos, *DHFR* overexpression partly reduced the expressions of *NKX2.5*, *MEF2C*, *TBX1*, *TBX20* and *Ptc-1*, and improved the expression of *Foxa2*. We also

found that *DHFR* overexpression accelerated proliferation and reduced apoptosis. These results indicated that *DHFR* not only had a positive effect on the expressions of *NKX2.5*, *MEF2C*, *TBX1*, *TBX20*, and *Ptc-1*, but could also promote cell proliferation and inhibit apoptosis.

Altogether, *DHFR* played crucial roles in the early embryonic development and the formation of heart and OFT, and could affect the expression of *NKX2.5*, *MEF2C*, *TBX20*, and *TBX1*. *DHFR* was also important for Hedgehog signaling, cell proliferation, and apoptosis.

Although this study provided some clues for the further investigation on the function of DHFR in embryonic and cardiac development, in light that the very significant abnormal formation of epiboly and body axis were observed at early stages, whether these events could be primary and cardiac malformations be secondary injury needs further study.

Acknowledgements

We thank several people for their contributions to this project. We acknowledge Dr Xuefei Liu and Dr Linxi Qian for assistances. We are also grateful to the members of the Prof. Houyan Song lab (Key Laboratory of Molecular Medicine, Ministry of Education, Fudan University) for advices and supports.

Funding

This work was supported by grants from the National Natural Science Foundation of China (30901472/H0204) and the Doctoral Fund of Ministry of Education of China (200802461111).

References

1 Obican SG, Finnell RH, Mills JL, Shaw GM and Scialli AR. Folic acid in early pregnancy: a public health success story. FASEB J 2010, 24: 4167–4174.
2 Hobbs CA, Cleves MA, Karim MA, Zhao W and MacLeod SL. Maternal folate-related gene environment interactions and congenital heart defects. Obstet Gynecol 2010, 116: 316–322.
3 Burgoon JM, Selhub J, Nadeau M and Sadler TW. Investigation of the effects of folate deficiency on embryonic development through the establishment of a folate deficient mouse model. Teratology 2002, 65: 219–227.
4 Goldmuntz E, Woyciechowski S, Renstrom D, Lupo PJ and Mitchell LE. Variants of folate metabolism genes and the risk of conotruncal cardiac defects. Circ Cardiovasc Genet 2008, 1: 126–132.
5 Mitchell LE, Long J, Garbarini J, Paluru P and Goldmuntz E. Variants of folate metabolism genes and risk of left-sided cardiac defects. Birth Defects Res A Clin Mol Teratol 2010, 88: 48–53.
6 Hernandez-Diaz S, Werler MM and Walker AM. Folic acid antagonists during pregnancy and the risk of birth defects. N Engl J Med 2000, 343: 1608–1614.
7 Bailey LB and Berry RJ. Folic acid supplementation and the occurrence of congenital heart defects, orofacial clefts, multiple births, and miscarriage. Am J Clin Nutr 2005, 81: 1213S–1217S.
8 Kalmbach RD, Choumenkovitch SF, Troen AP, Jacques PF, D'Agostino R and Selhub J. A 19-base pair deletion polymorphism in dihydrofolate reductase is associated with increased unmetabolized folic acid in plasma and decreased red blood cell folate. J Nutr 2008, 138: 2323–2327.
9 Vander Linden IJ, Nguyen U, Heil SG, Franke B, Vloet S, Gellekink H and den Heijer M, *et al*. Variation and expression of dihydrofolate reductase (DHFR) in relation to spina bifida. Mol Genet Metab 2007, 91: 98–103.
10 Sun SN, Gui YH, Wang YX, Qian LX, Jiang Q, Liu D and Song HY. Effect of dihydrofolate reductase gene knock-down on the expression of heart and neural crest derivatives expressed transcript 2 in zebrafish cardiac development. Chin Med J (Engl) 2007, 120: 1166–1171.
11 Sun S, Gui Y, Wang Y, Qian L, Liu X, Jiang Q and Song H. Effects of methotrexate on the development of heart and vessel in zebrafish. Acta Biochim Biophys Sin 2009, 41: 86–96.
12 Elliott DA, Solloway MJ, Wise N, Biben C, Costa MW, Furtado MB and Lange M, *et al*. A tyrosine-rich domain within homeodomain transcription factor Nkx2–5 is an essential element in the early cardiac transcriptional regulatory machinery. Development 2006, 133: 1311–1322.
13 Vincentz JW, Barnes RM, Firulli BA, Conway SJ and Firulli AB. Cooperative interaction of Nkx2.5 and Mef2c transcription factors during heart development. Dev Dyn 2008, 237: 3809–3819.
14 Xu H, Morishima M, Wylie JN, Schwartz RJ, Bruneau BG, Lindsay EA and Baldini A. Tbx1 has a dual role in the morphogenesis of the cardiac outflow tract. Development 2004, 31: 3217–3227.
15 Takeuchi JK, Mileikovskaia M, Koshiba-Takeuchi K, Heidt AB, Mori AD, Arruda EP and Gertsenstein M, *et al*. Tbx20 dose-dependently regulates transcription factor networks required for mouse heart and motoneuron development. Development 2005, 132: 2463–2474.
16 Goddeeris MM, Schwartz R, Klingensmith J and Meyers EN. Independent requirements for Hedgehog signaling by both the anterior heart field and neural crest cells for outflow tract development. Development 2007, 134: 1593–1604.
17 Kimmel CB, Ballard WW, Kimmel SR, Ullmann B and Schilling TF. Stages of embryonic development of the zebrafish. Dev Dyn 1995, 203: 253–310.
18 Wang YX, Qian LX, Yu Z, Jiang Q, Dong YX, Liu XF and Yang XY, *et al*. Requirements of myocyte-specific enhancer factor 2A in zebrafish cardiac contractility. FEBS Lett 2005, 79: 4843–4850.
19 Berdougo E, Coleman H, Lee DH, Stainier DY and Yelon D. Mutation of weak atrium/atrial myosin heavy chain disrupts atrial function and influences ventricular morphogenesis in zebrafish. Development 2003, 130: 6121–6129.
20 Benson DW, Silberbach GM, Kavanaugh-McHugh A, Cottrill C, Zhang Y, Riggs S and Smalls O, *et al*. Mutations in the cardiac transcription factor NKX2.5 affect diverse cardiac developmental pathways. J Clin Invest 1999, 104: 1567–1573.
21 Tanaka M, Chen Z, Bartunkova S, Yamasaki N and Izumo S. The cardiac homeobox gene Csx/Nkx2.5 lies genetically upstream of multiple genes essential for heart development. Development 1999, 126: 1269–1280.
22 Akazawa H and Komuro I. Cardiac transcription factor Csx/Nkx2–5: its role in cardiac development and diseases. Pharmacol Ther 2005, 107: 252–268.
23 Liu ZP, Nakagawa O, Nakagawa M, Yanagisawa H, Passier R, Richardson JA and Srivastava D, *et al*. CHAMP, a novel cardiac-specific helicase regulated by MEF2C. Dev Biol 2001, 234: 497–509.
24 Kelly RG and Papaioannou VE. Visualization of outflow tract development in the absence of Tbx1 using an FgF10 enhancer trap transgene. Dev Dyn 2007, 236: 821–828.

25 Morishima M, Yanagisawa H, Yanagisawa M and Baldini A. Ece1 and Tbx1 define distinct pathways to aortic arch morphogenesis. Dev Dyn 2003, 228: 95–104.
26 Nowotschin S, Liao J, Gage PJ, Epstein JA, Campione M and Morrow BE. Tbx1 affects asymmetric cardiac morphogenesis by regulating Pitx2 in the secondary heart field. Development 2006, 133: 1565–1573.
27 Stennard FA, Costa MW, Lai D, Biben C, Furtado MB, Solloway MJ and McCulley DJ, *et al*. Murine T-box transcription factor Tbx20 acts as a repressor during heart development, and is essential for adult heart integrity, function and adaptation. Development 2005, 132: 2451–2462.
28 Stennard FA, Costa MW, Elliott DA, Rankin S, Haast SJ, Lai D and McDonald LP, *et al*. Cardiac T-box factor Tbx20 directly interacts with Nkx2–5, GATA4, and GATA5 in regulation of gene expression in the developing heart. Dev Biol 2003, 262: 206–224.
29 Washington Smoak I, Byrd NA, Abu-Issa R, Goddeeris MM, Anderson R, Morris J and Yamamura K, *et al*. Sonic hedgehog is required for cardiac outflow tract and neural crest cell development. Dev Biol 2005, 283: 357–372.
30 Zhang XM, Ramalho-Santos M and McMahon AP. Smoothened mutants reveal redundant roles for Shh and Ihh signaling including regulation of L/R asymmetry by the mouse node. Cell 2001, 105: 781–792.
31 Schilling TF, Concordet JP and Ingham PW. Regulation of left–right asymmetries in the zebrafish by Shh and BMP4. Dev Biol 1999, 210: 277–287.